

# Observation of the new emission line at $\sim 3.5$ keV in the X-ray spectra of galaxies and galaxy clusters

D. A. Iakubovskiy\*

Discovery Center, Niels Bohr Institute, Blegdamsvej 17, Copenhagen, Denmark  
Bogolyubov Institute of Theoretical Physics, Metrologichna Str. 14-b, 03680, Kyiv, Ukraine

The detection of an unidentified emission line in the X-ray spectra of cosmic objects would be a ‘smoking gun’ signature for the particle physics beyond the Standard Model. More than a decade of its extensive searches results in several narrow faint emission lines reported at 3.5, 8.7, 9.4 and 10.1 keV. The most promising of them is the emission line at  $\sim 3.5$  keV reported in spectra of several nearby galaxies and galaxy clusters. Here I summarize its up-to-date status, overview its possible interpretations, including an intriguing connection with the radiatively decaying dark matter, and outline future directions for its studies.

**Key words:** X-rays: general, dark matter, line: identification

## INTRODUCTION

The origin of the *dark matter* – the major (yet of unknown origin) gravitating substance in the Universe [17, 51, 56, 59, 60, 62, 70, 71, 72, 78, 79, 84, 87, 122, 123, 137, 140, 143, 144, 151, 152, 155, 170, 179, 188] – still has to be revealed. If the dark matter is made of elementary particles, the latter should be massive (to form over-densities in process of gravitational collapse), long-lived (to be stable for at least the age of the Universe) and neutral with respect to strong and electromagnetic interactions (to be sufficiently ‘dark’). The only known massive, long-lived and neutral particles are the usual (left-handed) neutrinos, but they are too light to form small dark matter halos [171, 184]. As a result, the hypothesis of the dark matter particle implies an extension of the Standard Model of particle physics. Dozens of the Standard Model extensions have been proposed so far to contain a valid dark matter particle candidate. However, as Fig. 1 from [80] demonstrates, the masses of dark matter particle candidates and their interaction strengths with Standard Model particles cover a huge region of parameter space. This results in a large variety of observational methods developed to search for dark matter particles.

The specific example considered in this review is the *radiatively decaying dark matter*. If a dark matter particle interacts with electrically charged particles, it may<sup>1</sup> possess a radiative decay channel. If a

non-relativistic dark matter particle decays to a photon and another particle, a slight ( $v/c \lesssim 5 \times 10^{-3}$ ) Doppler broadening due to non-zero velocities of dark matter particles in halos would cause a narrow *dark matter decay line*. Such a decay line possesses several specific features allowing to robustly distinct it from the emission lines of astrophysical origin (see e. g. [64, 164]) or from instrumental line-like features:

- its position in energy is solely determined by the mass of the dark matter particle and the redshift of the dark matter halo (i. e. if one neglects the mass of other decay products, the line position is  $\frac{m_{\text{DM}}c^2}{2(1+z)}$ ), having different scaling with the halo redshift  $z$  as the instrumental line-like features;
- its intensity is proportional to *the dark matter column density*  $\mathcal{S}_{\text{DM}} = \int \rho_{\text{DM}} dl$ ; due to the different 3D distributions of the dark and visible matter, comparison of the new line intensity within the given object — as well as among among different objects — would allow to choose between its decaying dark matter and astrophysical origins;
- it is broadened with the characteristic velocity of the dark matter — different from that of visible matter.

\*iakubovskiy@nbi.ku.dk

<sup>1</sup>The widely-known examples where this is *not* the case are the dark matter particles as the *lightest* particles holding a new quantum number *conserved* by the Standard Model interactions, such as R-parity for super-symmetric models, Kaluza-Klein number for extra dimensions, etc. In this case, the dark matter decays are strictly forbidden by the special structure of the theory, and the main astrophysical effect for the dark matter particles is their *annihilation* with their antiparticles.

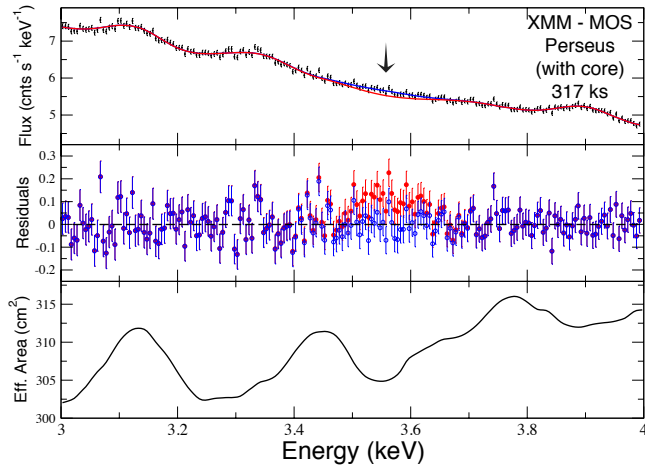


Fig. 1: The combined MOS spectrum of the Perseus cluster scaled to the 3-4 keV energy range. On top of the their best-fit model, the series of the single-bin residuals corresponding to the extra emission line at 3.57 keV are shown in red. (Adapted from Figure 7 in [45]).

The above-mentioned characteristics allow to *directly detect the radiatively decaying dark matter relying on the astrophysical measurements*. This motivates the extensive search for the new lines in X-ray spectra of cosmic objects proposed about 15 years ago [2, 3, 67], see Table 1. An example is the analysis of the line candidate at  $\sim 2.5$  keV initially reported in [112] in the X-ray spectrum of the Willman 1 dwarf spheroidal at  $2.5\sigma$  level. Further non-observation of this line candidate in the central part and outskirts of the Andromeda galaxy, Fornax and Sculptor dwarf spheroidal galaxies [41] excludes the decaying dark matter origin of the  $\sim 2.5$  keV signal at a high significance level (above  $14\sigma$ ). This result is further strengthened by the authors of [128] who reanalysed the same observations of Willman 1 as [112] (and did not find the  $\sim 2.5$  keV line) and the authors of [127] who analysed another dwarf spheroidal, Segue 1. Finally, [113] ruled out the dark matter origin of the  $\sim 2.5$  keV feature by observing Willman 1 with better statistics. The probable origin of the  $\sim 2.5$  keV line, according to [41], is purely instrumental, being the result of under-modelling of the time-variable soft proton background (see e.g. [106]) in some observations combined with an apparent dip at  $\sim 2.5$  keV in the effective area of existing X-ray instruments.

## OBSERVATIONAL EVIDENCE FOR THE LINE AT $\sim 3.5$ KEV

The new emission line at  $\sim 3.5$  keV was reported by two different groups [39, 45] in February 2014. In [45], the authors combine X-ray emission from the sample of nearby galaxy clusters observed by the Eu-

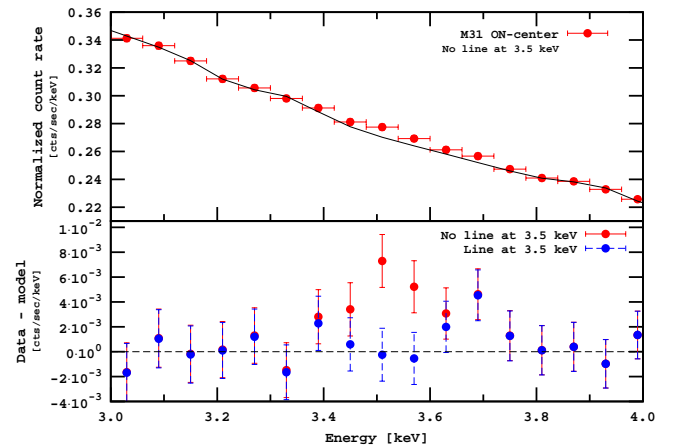


Fig. 2: The same as in Figure 1 but for the combined spectrum of Andromeda galaxy. (Adapted from Figure 1 in [39]).

ropean Photon and Imaging Camera (EPIC) [167, 172] on-board the *XMM-Newton* X-ray cosmic observatory [95] with the largest number of counts ( $>10^5$  counts for redshifts  $z < 0.1$  and  $>10^4$  counts for redshifts  $0.1 < z < 0.4$ ). The stacking is made in the cluster's rest frame. As a result, the emission from the instrumental lines is smeared out, while cosmic lines appear prominent. This method allows [45] to detect 28 emission lines of astrophysical origin in 2-10 keV band, much more than in individual galaxy clusters, see e.g. [61]. Apart from them, [45] identifies the new line located at  $3.57 \pm 0.02$  keV in *XMM-Newton*/MOS [167] cameras and at  $3.51 \pm 0.03$  keV in *XMM-Newton*/PN [172] camera at the level  $\gtrsim 10$  larger than predicted from the two complexes of nearby astrophysical emission lines located at 3.51 keV (K XVIII) and 3.62 keV (Ar XVII). The new line is also detected at  $> 3\sigma$  local significance in several different sub-samples of their combined *XMM-Newton*/EPIC cluster dataset, see e.g. Fig. 1, and in *Chandra*/ACIS spectrum of Perseus cluster, see Table 2 for details.

In [39] the new line at  $3.53 \pm 0.03$  keV in the central part of Andromeda galaxy (see Fig. 2) and in the outskirts of Perseus cluster is detected, see Table 2. [39] excluded the central part of the Perseus cluster (analysed in [45]) because of its rather complex structure in X-rays, so the two datasets used in [39, 45] are totally independent enhancing the statistical significance for the new line. Another important result of [39] is the radial dependence of the new line flux in Perseus that appears more consistent with the decaying dark matter profile than with the astrophysical emission.

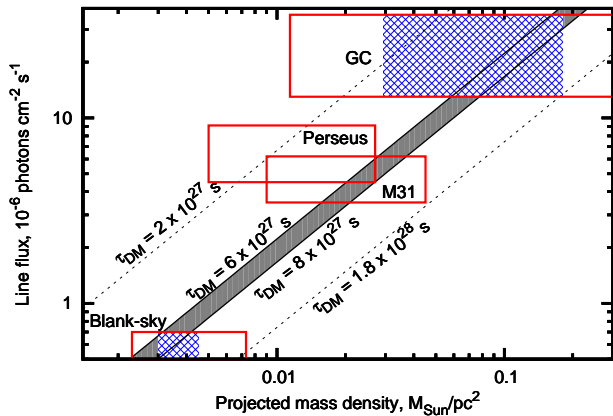


Fig. 3: The flux of the  $\sim 3.5$  keV line from the Galactic Centre, the Perseus cluster outskirts, the Andromeda galaxy, and the ‘blank sky’ dataset [39] as a function of the dark matter projected mass. Diagonal lines show the expected behaviour of the decaying dark matter signal for a given dark matter particle lifetime. The vertical sizes of the boxes are  $\pm 1\sigma$  statistical error on the line’s flux – or the  $2\sigma$  upper bound for the blank-sky dataset. The blue shaded regions show a particular Navarro-Frenk-White [132, 133] profile of the Milky Way [163], its horizontal size indicates uncertainties in the galactic disk modelling. The lifetime  $\tau_{\text{DM}} \sim (6-8) \times 10^{27}$  s is consistent with all datasets. New results from a prolonged Draco *XMM-Newton*/EPIC observation [98, 153] give controversial results: while [98] reports an exclusion of dark matter hypothesis at 99% level, the results of [153] claim that the values of  $\tau_{\text{DM}} \simeq (7-9) \times 10^{27}$  sec are still consistent with *all* existing observations. (Adapted from Figure 2 in [27]).

The encouraging results of [39, 45] have stimulated several groups to look at the other dark matter-dominated objects. The following searches report the presence of the line at  $\sim 3.5$  keV, see Table 3:

1. The identification of the line at  $\sim 3.5$  keV from the region of the Galactic Centre [27, 49, 97, 145]. Although it is unclear whether the detected line has an astrophysical origin (see the next section for detailed discussion), its explanation in terms of decaying dark matter is consistent with the previous new line detections, see [27, 115] for details.
2. The detection of the new line in *Suzaku*/XIS observations of the Perseus, Coma and Ophiuchus galaxy clusters [173]. While the subsequent study of *Suzaku*/XIS spectra in [169] did not reveal the new line at  $\sim 3.5$  keV in the central part of the Perseus cluster, another recent study in [77] does; however, its apparent discrepancy with the negative result of [169] is still unclear and has to be resolved further.

3. The detection of the new line at  $3.52 \pm 0.08$  keV observed in the X-ray spectra of 8 individual nearby galaxy clusters including Perseus and Coma [93].

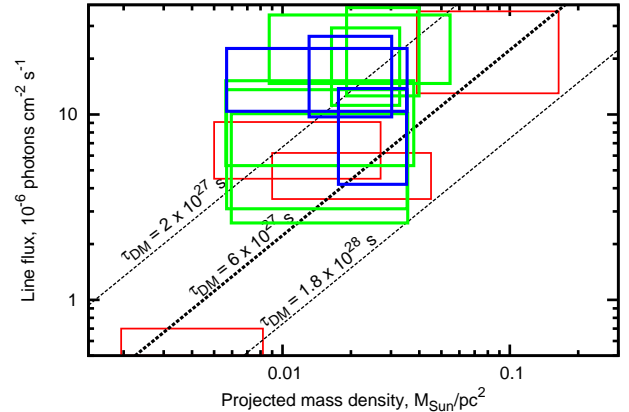


Fig. 4: The same as in Fig. 3 but over-plotted are the ranges for the  $> 2\sigma$  detections in MOS (green) and PN (magenta) cameras, see [93]. (Adapted from Figure 2 in [93]).

In summary, positive detections of the new line listed in Tables 2 and 3 support the hypothesis of the radiatively decaying dark matter implying its lifetime is  $\tau_{\text{DM}} \simeq (6-8) \times 10^{27}$  s [27, 93, 153].

On the contrary, the following studies do not detect the  $\sim 3.5$  keV line putting the upper bounds on its flux:

1. The central part of the Virgo cluster observed by *Chandra*/ACIS [45], *Suzaku*/XIS [173] and *XMM-Newton*/EPIC [93], as well as other 10 galaxy clusters from [93].
2. Combined spectrum from dwarf spheroidal galaxies [120].
3. Outskirts of galaxies [9, 39, 91].
4. Combined blank-sky observations [39, 159].
5. Prolonged *XMM-Newton*/EPIC observations of the Draco dwarf spheroidal galaxy [98, 153]; although [153] reports a line-like excess at  $3.54 \pm 0.06$  keV with  $\Delta\chi^2 = 5.3$  in PN camera, see Table 2, this finding is not supported by an independent analysis of [98] and is not accompanied with a similar excess in Draco spectra seen by MOS camera [98, 153].

At the moment, it is unclear whether these negative searches rule out the decaying dark matter hypothesis for this new line. While the bounds obtained in [120] are mildly consistent with the decaying dark

matter origin of the detections in [39, 45], the results of [9] formally exclude the decaying dark matter hypothesis of the origin of the  $\sim 3.5$  keV line imposing a very strict  $3\sigma$  bound,  $\tau_{\text{DM}} > 1.8 \times 10^{28}$  s. However, taking into account the systematic effects in the spectra (e.g. causing significant negative residuals) obtained in [9] and the apparent uncertainty in the used dark matter distributions [40] would result in much weaker bound. For instance,  $\tau_{\text{DM}} \gtrsim 3.5 \times 10^{27}$  s is reported in [94] using the stacked dataset of nearby galaxies with comparable exposure from [91] — still consistent with existing detections. The uncertainty in the dark matter distributions also helps to reconcile the results of the other negative searches [89, 159, 182] with the  $\sim 3.5$  keV line detections using the decaying dark matter paradigm. There is also no clarity with the new prolonged ( $\sim 1.4$  Ms) *XMM-Newton*/EPIC observation of the Draco dwarf spheroidal galaxy — the object having both well-measured dark matter distribution [82] and proven low X-ray background [99, 115, 120, 146]. While [98] reports an exclusion of dark matter hypothesis at 99% level having  $2\sigma$  upper bound on the radiative dark matter decay lifetime of  $\tau_{\text{DM}} > 2.7 \times 10^{28}$  s, the results of [153] suggest  $\tau_{\text{DM}} \simeq (7 - 9) \times 10^{27}$  s — the value still compatible with all existing observations.

### “STANDARD” EXPLANATIONS OF THE LINE AT $\sim 3.5$ KEV

There are three possible “standard” explanations of the new line detections at  $\sim 3.5$  keV:

1. statistical fluctuations;
2. general-type systematic effects;
3. astrophysical emission line.

With recent increase of positive detections reported by [93], it is very hard to explain *all* of the detections with pure statistical fluctuations. Nevertheless, statistical fluctuations may be responsible for the new line detections or non-detections in *some* individual objects, as well as for variations of the detected line position up to  $\sim 110$  eV [93], see Fig. 5 — the effect that should be properly taken into account when searching for the new line (unlike [9, 120, 173]).

The systematic origin of the line is carefully investigated because of the previous study of the line-like residual at  $\sim 2.5$  keV in the Willman 1 dwarf spheroidal, see the ‘Introduction’ section for details. However, the explanation of the  $\sim 3.5$  keV line with

the general-type systematics suggested in [97] is unlikely. For example, its position (in the frame of emitting object) remains remarkably constant with the redshift [39, 45, 93], see Fig. 5, which cannot be explained by simple systematics. The line is also independently detected by five detectors on-board three cosmic missions, see Tables 2 and 3. Finally, similar feature of systematic origin should have been detected in the blank-sky dataset [39], and should have different radial behaviour in the outskirts of the Perseus cluster [39, 77].

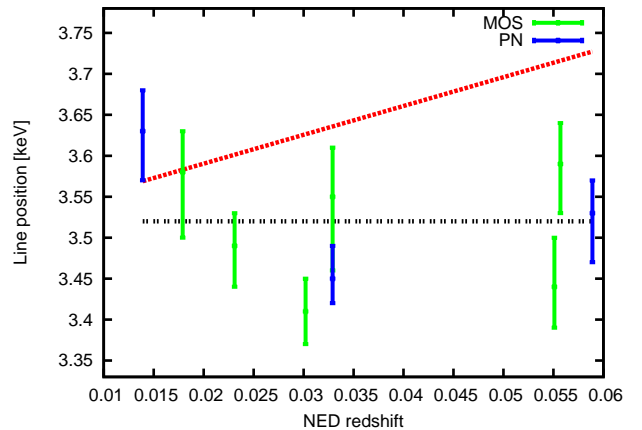


Fig. 5: The position of new line detected in [93] (in the frame of emitting galaxy cluster) as a function of the cluster redshift. The red and black dashed lines show the expected behaviour in case of purely systematic and cosmic line origins (assuming the line position 3.52 keV in the detector frame expected from [39, 27]), respectively (Adapted from Figure 3 in [93]).

On the other hand, the explanation of the new line with the K XVIII line complex at  $\sim 3.5$  keV suggested by [97] (see also an extensive discussion in [28, 45, 46, 96]) is still possible, at least for the Galactic Centre region and galaxy clusters, contrary to the initial claims of [39, 45]. The reason is that the emission flux from the K XVIII line complex at  $\sim 3.51$  keV suggested by [97] is highly uncertain due to large uncertainties of the Potassium abundance, see e.g. [139, 150] for a potential<sup>2</sup> level of uncertainty. Moreover, unlike other possible emission lines of astrophysical origin near  $\sim 3.5$  keV (such as Cl XVII lines at 3.51 keV found largely subdominant in the Galactic Centre region [97] and in galaxy clusters [46]), K XVIII line complex does not have stronger counterparts at other energies and can hardly be excluded by the measurements of other lines, the strongest of them is the K XIX line com-

<sup>2</sup>The results of [139] indicate an order of magnitude over-abundance of Potassium in the solar corona compared to the solar photosphere. Based on this result, [139] suggested that the Potassium abundance in hot plasma in galaxies and galaxy clusters may have also been enhanced compared to the solar photospheric values. However, because at the moment there is no established mechanism that could effectively provide such an enhancement, the results of [139] only indicate the *potential* level of uncertainty, similar to the measurements in [150].

plex at 3.71 keV of comparable strength [92]. The same is true about the charge exchange of S XVI ions recently suggested by [86].

An alternative approach is to study the *line morphology*. At the moment, two different methods have been used. The first method [39, 45] is to split the region covered by some astrophysical sources into several independent subregions, large enough to detect the line in each of them, and to model their spectra separately looking for a line-like excess in each of subregions. As a result, in [45] it was shown that the  $\sim 3.5$  keV line in the Perseus cluster is somewhat more concentrated compared to decaying dark matter distributed according to the Navarro-Frenk-White [132, 133] profile. By studying the  $\sim 3.5$  keV line emission from the Perseus cluster outskirts, in [39] it was obtained that such distribution is better consistent with the radiatively decaying dark matter distributed according to the well-established Navarro-Frenk-White profile than with the astrophysical continuum emission distributed according to the isothermal  $\beta$ -model of [50]. The recent detailed study [77] confirms this result and expands it to the central region of the Perseus cluster.

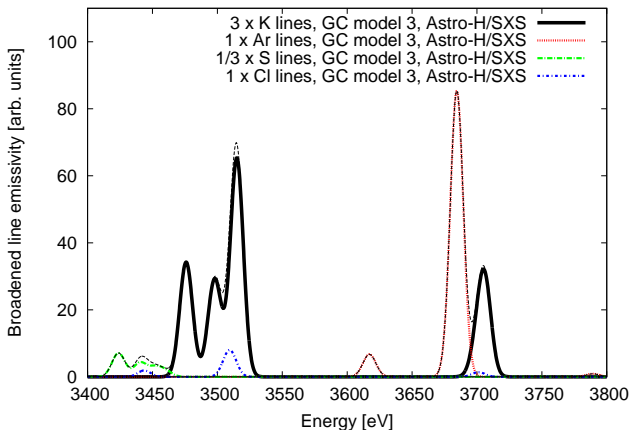


Fig. 6: Line emissivities (in arbitrary units) broadened with energy resolution of Soft X-ray Spectrometer (SXS) on-board *Hitomi* (former *Astro-H*),  $\sigma_{SXS} = 5$  eV, as functions of energy for three-component model of [97] of Galactic Centre. The relative S, Ar, Cl and K abundances are set to 1/3 : 1 : 1 : 3, according to Sec. 2.2 of [97]. Thin dashed line shows the total line emissivity (Adapted from Figure 2 in [92]).

The second method to study the line morphology [49] deals with the spatial distribution of the ‘line plus continuum’ X-ray emission in the Perseus cluster and the Galactic Centre region with further eliminating the continuum component by either as-

suming it is spatially smooth or cross-correlating the ‘line plus continuum’ images in several energy bands (including those dominated by the astrophysical line emission). By using the second method, the authors of [49] show that adding the decaying dark matter distribution from a *smooth* dark matter profile (Navarro-Frenk-White, Einasto, Burkert) does not improve the fit quality in both objects, and demonstrate that distribution of the events in the 3.45–3.6 keV bands correlates with that in the energy bands of strong astrophysical emission, rather than with that in line-free energy bands. Based on these findings, [49] claims the exclusion of the decaying dark matter origin of 3.5 keV in the Galactic Centre and the Perseus cluster.

To ultimately check the astrophysical origin of the  $\sim 3.5$  keV line, new observations with high-resolution imaging<sup>3</sup> spectrometers such as Soft X-ray Spectrometer (SXS) [130] on-board the recently launched *Hitomi*<sup>4</sup> (former *Astro-H*) mission [168], *Micro-X* sounding rocket experiment [73] and the X-ray Integral Field Unit (X-IFU) [14, 142] on-board the planned *Athena* mission [15, 131], are planned. If the position of the new line incidentally coincides with that of the K XVIII line complex, a more detailed study of the ratios of the Potassium line emissivities will be essential to finally check the astrophysical origin of the new line, see Fig. 6 for details.

## OTHER EXTRA LINE

### CANDIDATES IN X-RAY RANGE

Although the line at  $\sim 3.5$  keV receives the largest attention of the community, there are three other line candidates in X-rays which origin is also not established:

1. According to [141], intensity of the Fe XXVI Ly $\gamma$  line at 8.7 keV observed in *Suzaku*/XIS spectrum of the Milky Way centre [103] cannot be explained by the standard ionization and recombination processes and dark matter decay may be a possible explanation of this excess.
2. According to Sec. 1.4 of [104], two faint extra line-like excesses at 9.4 and 10.1 keV are detected in the combined *Suzaku*/XIS spectrum of the Galactic Bulge region. Notably, positions of these excesses do not coincide with any bright<sup>5</sup> astrophysical or instrumental line and their intensities can be explained in frames of decaying dark matter origin, see right Fig. 8 of [104].

<sup>3</sup> *Grating* spectrometers such as *Chandra*/HETGS [48] have excellent spectral resolution for *point* sources; however, for extended ( $\gtrsim 1$  arcmin) sources their spectral resolution usually degrades to that of existing imaging spectrometers, see e.g. [65].

<sup>4</sup> Although *Hitomi* is now broken apart, it had observed Perseus cluster before becoming non-operational [88, 101].

<sup>5</sup> The newest available atomic database AtomDB v.3.0.2 [75] contains several faint Ni XXVI – Ni XXVIII emission lines at 10.02–10.11 keV.

## POSSIBLE IMPLICATIONS FOR NEW PHYSICS

If none of the “conventional” explanations discussed in the previous sections were valid, the existence of the new line at  $\sim 3.55$  keV would be an indication of a new physics beyond the Standard Model.

Historically, the first model discussed in connection with  $\sim 3.5$  keV detection is the neutrino minimal extension of the Standard Model with three right-handed (sterile) neutrinos (the  $\nu$ MSM) [12, 43]. In this model, the lightest sterile neutrino with the mass in keV range forms the bulk of dark matter while the two heavier sterile neutrinos are responsible for the two other established phenomena beyond the Standard Model – neutrino oscillations and generation of asymmetry between baryons and anti-baryons in early Universe. Sterile neutrinos decay possesses the 2-body radiative channel  $N \rightarrow \gamma + \nu$ , so the observation of  $\sim 3.5$  keV decay line would imply the existence of light sterile neutrino dark matter particles with mass  $\sim 7.1$  keV. The simplest production scenario of sterile neutrino dark matter — via the non-resonant oscillations of the usual (active) neutrinos in the early Universe [1, 2, 3, 11, 66, 67] — is already excluded by the combination of the X-ray measurements [30], measurements of the Ly $\alpha$  forest [31, 32, 160, 176, 177, 178] and the phase-space bound from dwarf spheroidal galaxies [10, 38, 85, 161, 171]. The realistic scenario of the dark matter production within the  $\nu$ MSM now involves the resonant oscillations of active neutrinos in hot primordial plasma with the significant lepton asymmetry generated by decays of heavier sterile neutrinos [4, 83, 108, 162, 174]. The parameters of the observed  $\sim 3.5$  keV line are consistent with the  $\nu$ MSM predictions, see Fig. 7 for details. Because the interaction of sterile neutrino dark matter with the Standard Model particles is orders of magnitude weaker than that of ordinary neutrinos, its prospects for direct detection in a particle physics experiment are very far from the existing experimental technique, see [6, 68, 110, 111, 126]. To confirm the  $\nu$ MSM, a search for heavier sterile neutrinos in the GeV range is needed, handled by e. g. the planned Search for Hidden Particles (*SHiP*) experiment [7, 21] and the Future electron-positron  $e^+e^-$  Circular Collider (*FCC-ee*) [19].

However, the confirmation of the decaying dark matter origin of the new line does not imply the existence of  $\nu$ MSM sterile neutrinos as there are plenty of other alternatives which can potentially explain the  $\sim 3.55$  keV line, see e. g. [6, 27, 94] and the references therein. Differences among these models can be further probed by:

- changes in the new line morphology because of the non-negligible initial dark matter velocities, see e. g. [117, 119];

- other astrophysical and cosmological tests, see e. g. [4, 23, 24, 25, 38, 44, 90, 100, 109, 116, 118, 124, 154, 156, 157, 175, 180];
- search for the “smoking gun” signatures in the future dedicated particle physics experiments, such as *SHiP* [7, 21] and *FCC-ee* [19] experiments.

Recently proposed alternatives to the radiatively decaying dark matter include: the decay of excited dark matter states [18, 20, 53, 54, 55, 63, 74, 138, 158], annihilating dark matter [13, 69, 76, 121], dark matter decaying into the axion-like particles with further conversion to photons in a magnetic field [8, 16, 52, 57, 58]. These models predict the *substantial* difference in the  $\sim 3.5$  keV line morphology compared to the radiatively decaying dark matter. For example, the spatial distributions of the new line in these models should be more concentrated towards the centres of the dark matter-dominated objects compared to radiatively decaying dark matter, e. g. due to larger dark matter density (for excited and annihilating dark matter) or larger magnetic fields (for magnetic field conversion of axion-like particles). Further non-observation of the  $\sim 3.5$  keV line in the outskirts of the dark matter-dominated objects would argue in favour of these models.

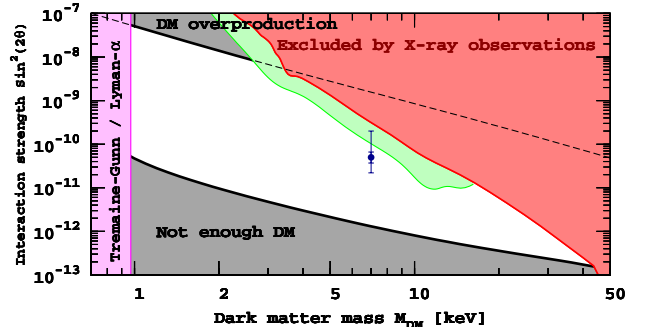


Fig. 7: Constraints on sterile neutrino dark matter within the  $\nu$ MSM model [12, 43]. In every point in the white region sterile neutrinos constitute 100% of dark matter and their properties agree with the existing bounds. The blue point corresponds to the observed line from the Andromeda galaxy, while the error bars indicate the statistical errors (thick) and uncertainty in the dark matter distribution at the central part of the Andromeda galaxy (thin) (Adapted from Figure 4 in [39]).

## CONCLUSION AND FUTURE DIRECTIONS

The origin of the new emission line at  $\sim 3.5$  keV reported in [27, 39, 45, 93, 173] remains unexplained. The observed properties of the new line are consistent with the radiatively decaying dark matter as well as the other interesting scenarios (such as exciting dark matter, annihilating dark matter and the

dark matter decaying into axion-like particles further converted in cosmic magnetic fields) motivated by various particle physics extensions of the Standard Model. In case of the radiatively decaying dark matter, further detections would lead to the direct detection of the new physics. Specially dedicated observations using the existing X-ray missions (such as *XMM-Newton*, *Chandra*, *Suzaku*) still allow for such detections although one should take special care of the various systematic effects that could mimic or hide the new line.

The alternative is to use new better instruments. The basic requirements for such instruments — higher *grasp* (the product of field-of-view and effective area) and better *spectral resolution* — were first formulated in [26]. Both the soft X-ray Spectrometer [130] on-board the new X-ray mission *Hitomi* (former *Astro-H*) [102, 168] and the planned *Micro-X* sounding rocket experiment [73] meet only the second requirement having the energy resolution by an order of magnitude better ( $\sim 5$  eV) than existing imaging spectrometers. Before being broken apart, *Hitomi* has already observed the Perseus cluster [101]. It was expected [45] that such an observation would have allowed *Hitomi* to precisely determine the new line position in the brightest objects with the prolonged observations and to detect the KXIX emission line complex at  $\sim 3.71$  keV. Another possible option is to resolve the intrinsic width of the new line because of its Doppler broadening in galaxies and galaxy clusters [45, 166]. As a result, *Hitomi*/SXS is able to check whether the new line comes from the new physics or from the (anomalously enhanced) astrophysical emission. The same is expected from the *Micro-X* rocket-based microcalorimeter (to be launched in 2017) which will observe the central region of our Galaxy. Another possibility is to use the planned *eROSITA* instrument on-board *Spektrum-Röntgen-Gamma* mission [125] and the planned *LOFT* mission [187] whose high grasp and moderate energy resolution would allow to detect the new line at much smaller intensities [134, 186]. Finally, an “ultimate” imaging spectrometer proposed in e. g. [29] (an example is the X-ray Integral Field Unit (X-IFU) [14, 142] on-board the planned *Athena* mission [15, 131]) would reveal the detailed morphology structure of the  $\sim 3.5$  keV line [135].

## ACKNOWLEDGEMENT

This work was supported by a research grant from VILLUM FONDEN. The author also acknowledges partial support from the Swiss National Science Foundation grant SCOPE IZ7370-152581, the Program of Cosmic Research of the National Academy of Sciences of Ukraine, the State Fund for Fundamental Research of Ukraine and the State Programme of Implementation of the Grid Technology in Ukraine during the early stages of this work.

## REFERENCES

- [1] Abazajian K. 2006, Phys. Rev. D, 73, 063506
- [2] Abazajian K., Fuller G. M. & Patel M. 2001, Phys. Rev. D, 64, 023501
- [3] Abazajian K., Fuller G. M. & Tucker W. H. 2001, ApJ, 562, 593
- [4] Abazajian K. N. 2014, Phys. Rev. Lett., 112, 161303
- [5] Abazajian K. N., Markevitch M., Koushiappas S. M. & Hickox R. C. 2007, Phys. Rev. D, 75, 063511
- [6] Adhikari R., Agostini M., Ky N. A. et al. 2016, [arXiv:1602.04816]
- [7] Alekhin S., Altmannshofer W., Asaka T. et al. 2015, [arXiv:1504.04855]
- [8] Alvarez P. D., Conlon J. P., Day F. V., Marsh M. C. D. & Rummel M. 2015, JCAP, 4, 013
- [9] Anderson M. E., Churazov E. & Bregman J. N. 2015, MNRAS, 452, 3905
- [10] Angus G. W. 2010, JCAP, 3, 026
- [11] Asaka T., Laine M. & Shaposhnikov M. 2006, J. High Energy Phys., 6, 053
- [12] Asaka T. & Shaposhnikov M. 2005, Phys. Lett. B, 620, 17
- [13] Baek S., Ko P. & Park W.-I. 2014, [arXiv:1405.3730]
- [14] Barret D., den Herder J. W., Piro L. et al. 2013, [arXiv:1308.6784]
- [15] Barret D., Nandra K., Barcons X. et al. 2013, in ‘*SF2A-2013: Proc. the Annual meeting of the French Society of Astronomy and Astrophysics*’, eds.: Cambresy L., Martins F., Nuss E. & Palacios A., 447
- [16] Berg M., Conlon J. P., Day F. et al. 2016, [arXiv:1605.01043]
- [17] Bergström L. 2000, Reports on Progress in Physics, 63, 793
- [18] Berlin A., DiFranzo A. & Hooper D. 2015, Phys. Rev. D, 91, 075018
- [19] Blondel A., Graverini E., Serra N. & Shaposhnikov M., for the FCC-ee study team. 2014, [arXiv:1411.5230]
- [20] Boddy K. K., Feng J. L., Kaplinghat M., Shadmi Y. & Tait T. M. P. 2014, Phys. Rev. D, 90, 095016
- [21] Bonivento W., Boyarsky A., Dijkstra H. et al. 2013, [arXiv:1310.1762]
- [22] Borriello E., Paolillo M., Miele G., Longo G. & Owen R. 2012, MNRAS, 425, 1628
- [23] Bose S., Frenk C. S., Jun H., Lacey C. G. & Lovell M. R. 2016, [arXiv:1605.03179]
- [24] Bose S., Hellwing W. A., Frenk C. S. et al. 2015, [arXiv:1507.01998]
- [25] Bose S., Hellwing W. A., Frenk C. S. et al. 2016, [arXiv:1604.07409]
- [26] Boyarsky A., den Herder J., Neronov A. & Ruchayskiy O. 2007, Astropart. Phys., 28, P. 303–311.
- [27] Boyarsky A., Franse J., Iakubovskiy D. & Ruchayskiy O. 2014, [arXiv:1408.2503]
- [28] Boyarsky A., Franse J., Iakubovskiy D. & Ruchayskiy O. 2014, [arXiv:1408.4388]
- [29] Boyarsky A., Iakubovskiy D. & Ruchayskiy O. 2012, Physics of the Dark Universe, 1, 136
- [30] Boyarsky A., Iakubovskiy D., Ruchayskiy O. & Sav-

- chenko V. 2008, MNRAS, 387, 1361
- [31] Boyarsky A., Lesgourgues J., Ruchayskiy O. & Viel M. 2009, JCAP, 5, 12
- [32] Boyarsky A., Lesgourgues J., Ruchayskiy O. & Viel M. 2009, Phys. Rev. Lett., 102, 201304
- [33] Boyarsky A., Malyshev D., Neronov A. & Ruchayskiy O. 2008, MNRAS, 387, 1345
- [34] Boyarsky A., Neronov A., Ruchayskiy O. & Shaposhnikov M. 2006, MNRAS, 370, 213
- [35] Boyarsky A., Neronov A., Ruchayskiy O. & Shaposhnikov M. 2006, Phys. Rev. D, 74, 103506
- [36] Boyarsky A., Neronov A., Ruchayskiy O., Shaposhnikov M. & Tkachev I. 2006, Phys. Rev. Lett., 97, 261302
- [37] Boyarsky A., Nevalainen J. & Ruchayskiy O. 2007, A&A, 471, 51
- [38] Boyarsky A., Ruchayskiy O. & Iakubovskiy D. 2009, JCAP, 3, 5
- [39] Boyarsky A., Ruchayskiy O., Iakubovskiy D. & Franse J. 2014, Phys. Rev. Lett., 113, 251301
- [40] Boyarsky A., Ruchayskiy O., Iakubovskiy D., Maccio' A. V. & Malyshev D. 2009, [arXiv:0911.1774]
- [41] Boyarsky A., Ruchayskiy O., Iakubovskiy D. et al. 2010, MNRAS, 407, 1188
- [42] Boyarsky A., Ruchayskiy O. & Markevitch M. 2008, ApJ, 673, 752
- [43] Boyarsky A., Ruchayskiy O. & Shaposhnikov M. 2009, Ann. Rev. Nucl. Particle Science, 59, 191
- [44] Bozek B., Boylan-Kolchin M., Horiuchi S. et al. 2015, [arXiv:1512.04544]
- [45] Bulbul E., Markevitch M., Foster A. et al. 2014, ApJ, 789, 13
- [46] Bulbul E., Markevitch M., Foster A. R. et al. 2014, [arXiv:1409.4143]
- [47] Bulbul E., Markevitch M., Foster A. et al. 2016, [arXiv:1605.02034]
- [48] Canizares C. R., Davis J. E., Dewey D. et al. 2005, PASP, 117, 1144
- [49] Carlson E., Jeltema T. & Profumo S. 2015, JCAP, 2, 009
- [50] Cavaliere A. & Fusco-Femiano R. 1976, A&A, 49, 137
- [51] Chemin L., Carignan C. & Foster T. 2009, ApJ, 705, 1395
- [52] Cicoli M., Conlon J. P., Marsh M. C. D. & Rummel M. 2014, Phys. Rev. D, 90, 023540
- [53] Cline J. M., Frey A. R. 2014, Phys. Rev. D, 90, 123537
- [54] Cline J. M., Frey A. R. 2014, JCAP, 10, 013
- [55] Cline J. M., Liu Z., Moore G. D., Farzan Y. & Xue W. 2014, Phys. Rev. D, 89, 121302
- [56] Cocco L., Gerhard O., Arnaboldi M. et al. 2009, MNRAS, 394, 1249
- [57] Conlon J. P. & Day F. V. 2014, JCAP, 11, 033
- [58] Conlon J. P. & Powell A. J. 2015, JCAP, 1, 019
- [59] Corbelli E. 2003, MNRAS, 342, 199
- [60] Corbelli E., Lorenzoni S., Walterbos R., Braun R. & Thilker D. 2010, A&A, 511, A89
- [61] de Plaa J., Werner N., Bleeker J. A. M. et al. 2007, A&A, 465, 345
- [62] Dekel A., Stoehr F., Mamon G. A. et al. 2005, Nature, 437, 707
- [63] D'Eramo F., Hambleton K., Profumo S. & Stefaniak T. 2016, [arXiv:1603.04859]
- [64] Dere K. P., Landi E., Mason H. E., Monsignori Fossi B. C. & Young P. R. 1997, A&AS, 125, 149
- [65] Dewey D. 2002, in 'High Resolution X-ray Spectroscopy with XMM-Newton and Chandra', ed.: Branduardi-Raymont G.
- [66] Dodelson S. & Widrow L. M. 1994, Phys. Rev. Lett., 72, 17
- [67] Dolgov A. D. & Hansen S. H. 2002, Astropart. Phys., 16, 339
- [68] Dragoun O. & Vénos D. 2015, [arXiv:1504.07496]
- [69] Dudas E., Heurtier L. & Mambrini Y. 2014, Phys. Rev. D, 90, 035002
- [70] Einasto J. 2009, [arXiv:0901.0632]
- [71] Einasto J. & Einasto M. 2000, in 'IAU Colloq. 174: Small Galaxy Groups', eds.: Valtonen M. J. & Flynn C., 360
- [72] Evrard A. E., Metzler C. A. & Navarro J. F. 1996, ApJ, 469, 494
- [73] Figueroa-Feliciano E., Anderson A. J., Castro D. et al. 2015, [arXiv:1506.05519]
- [74] Finkbeiner D. P. & Weiner N. 2014, [arXiv:1402.6671]
- [75] Foster A., Smith R. K., Brickhouse N. S. et al. 2014, in 'AAS/High Energy Astrophysics Division', 115.06
- [76] Frandsen M. T., Sannino F., Shoemaker I. M. & Svendsen O. 2014, JCAP, 5, 033
- [77] Franse J., Bulbul E., Foster A. et al. 2016, [arXiv:1604.01759]
- [78] Frenk C. S. & White S. D. M. 2012, Annalen der Physik, 524, 507
- [79] Fu L., Semboloni E., Hoekstra H. et al. 2008, A&A, 479, 9
- [80] Gardner S. & Fuller G. M. 2013, Progress in Particle and Nuclear Physics, 71, 167
- [81] Garmire G. P., Bautz M. W., Ford P. G., Nousek J. A. & Ricker G. R. Jr. 2003, in 'X-Ray and Gamma-Ray Telescopes and Instruments for Astronomy', eds.: Truemper J. E. & Tananbaum H. D., 28
- [82] Geringer-Sameth A., Koushiappas S. M. & Walker M. 2015, ApJ, 801, 74
- [83] Ghiglieri J., Laine M. 2015, J. High Energy Phys., 11, 171
- [84] Gilmore G., Wilkinson M. I., Wyse R. F. G. et al. 2007, ApJ, 663, 948
- [85] Gorbunov D., Khmel'nitsky A. & Rubakov V. 2008, JCAP, 0810, 041
- [86] Gu L., Kaastra J., Raassen A. J. J. et al. 2015, A&A, 584, L11
- [87] Hinshaw G., Larson D., Komatsu E. et al. 2013, ApJs, 208, 19
- [88] Hitomi Collaboration: Aharonian F., Akamatsu H. et al. 2016, Nature, 535, 117
- [89] Horiuchi S., Humphrey P. J., Oñorbe J. et al. 2014, Phys. Rev. D, 89, 025017
- [90] Horiuchi S., Ng K. C. Y., Gaskins J. M., Smith M. & Preece R. 2015, [arXiv:1502.03399]
- [91] Iakubovskiy D. 2013, 'Constraining properties of dark



- matter particles using astrophysical data*, Ph.D. thesis, Instituut-Lorentz for Theoretical Physics
- [92] Iakubovskiy D. 2015, MNRAS, 453, 4097
- [93] Iakubovskiy D., Bulbul E., Foster A. R., Savchenko D. & Sadova V. 2015, [arXiv:1508.05186]
- [94] Iakubovskiy D. A. 2014, Advances in Astronomy and Space Physics, 4, 9
- [95] Jansen F., Lumb D., Altieri B. et al. 2001, A&A, 365, L1
- [96] Jeltema T. & Profumo S. 2014, [arXiv:1411.1759]
- [97] Jeltema T. & Profumo S. 2015, MNRAS, 450, 2143
- [98] Jeltema T. & Profumo S. 2016, MNRAS, 458, 3592
- [99] Jeltema T. E. & Profumo S. 2008, ApJ, 686, 1045
- [100] Kamada A., Inoue K. T. & Takahashi T. 2016, [arXiv:1604.01489]
- [101] Kelley R. L. & Mitsuda K. 2016, in *'AAS/High Energy Astrophysics Division'*, 206.02
- [102] Kitayama T., Bautz M., Markevitch M. et al. 2014, [arXiv:1412.1176]
- [103] Koyama K., Hyodo Y., Inui T. et al. 2007, PASJ, 59, 245
- [104] Koyama K., Kataoka J., Nobukawa M. et al. 2014, [arXiv:1412.1170]
- [105] Koyama K., Tsunemi H., Dotani T. et al. 2007, PASJ, 59, 33
- [106] Kuntz K. D. & Snowden S. L. 2008, A&A, 478, 575
- [107] Kusenko A., Loewenstein M. & Yanagida T. T. 2013, Phys. Rev. D, 87, 043508
- [108] Laine M. & Shaposhnikov M. 2008, JCAP, 6, 31
- [109] Li R., Frenk C. S., Cole S. et al. 2016, MNRAS, 460, 363
- [110] Liao W. 2010, Phys. Rev. D, 82, 073001
- [111] Liao W., Wu X.-H. & Zhou H. 2014, Phys. Rev. D, 89, 093017
- [112] Loewenstein M. & Kusenko A. 2010, ApJ, 714, 652
- [113] Loewenstein M. & Kusenko A. 2012, ApJ, 751, 82
- [114] Loewenstein M., Kusenko A. & Biermann P. L. 2009, ApJ, 700, 426
- [115] Lovell M. R., Bertone G., Boyarsky A., Jenkins A. & Ruchayskiy O. 2015, MNRAS, 451, 1573
- [116] Lovell M. R., Bose S., Boyarsky A. et al. 2015, [arXiv:1511.04078]
- [117] Lovell M. R., Frenk C. S., Eke V. R. et al. 2014, MNRAS, 439, 300
- [118] Ludlow A. D., Bose S., Angulo R. E. et al. 2016, [arXiv:1601.02624]
- [119] Macciò A. V., Ruchayskiy O., Boyarsky A. & Muñoz-Cuartas J. C. 2013, MNRAS, 428, 882
- [120] Malyshev D., Neronov A. & Eckert D. 2014, Phys. Rev. D, 90, 103506
- [121] Mambrini Y. & Toma T. 2015, [arXiv:1506.02032]
- [122] Massey R., Kitching T. & Richard J. 2010, Reports on Progress in Physics, 73, 086901
- [123] Massey R., Rhodes J., Ellis R. et al. 2007, Nature, 445, 286
- [124] Merle A., Schneider A. 2015, Phys. Lett. B, 749, 283
- [125] Merloni A., Predehl P., Becker W. et al. 2012, [arXiv:1209.3114]
- [126] Mertens S., Dolde K., Korzeczek M. et al. 2015, Phys. Rev. D, 91, 042005
- [127] Mirabal N. 2010, MNRAS, 409, L128
- [128] Mirabal N. & Nieto D. 2010, [arXiv:1003.3745]
- [129] Mitsuda K., Bautz M., Inoue H. et al. 2007, PASJ, 59, 1
- [130] Mitsuda K., Kelley R. L., Akamatsu H. et al. 2014, SPIE Conf. Ser., 9144, 2
- [131] Nandra K., Barret D., Barcons X. et al. 2013, [arXiv:1306.2307]
- [132] Navarro J. F., Frenk C. S. & White S. D. M. 1996, ApJ, 462, 563
- [133] Navarro J. F., Frenk C. S. & White S. D. M. 1997, ApJ, 490, 493
- [134] Neronov A., Boyarsky A., Iakubovskiy D. & Ruchayskiy O. 2014, Phys. Rev. D, 90, 123532
- [135] Neronov A. & Malyshev D. 2015, [arXiv:1509.02758]
- [136] Ng K. C. Y., Horiuchi S., Gaskins J. M., Smith M. & Preece R. 2015, Phys. Rev. D, 92, 043503
- [137] Noordermeer E., van der Hulst J. M., Sancisi R., Swaters R. S. & van Albada T. S. 2007, MNRAS, 376, 1513
- [138] Okada H. & Toma T. 2014, Phys. Lett. B, 737, 162
- [139] Phillips K. J. H., Sylwester B. & Sylwester J. 2015, ApJ, 809, 50
- [140] Planck Collaboration: Ade P. A. R., Aghanim N. et al. 2015, [arXiv:1502.01589]
- [141] Prokhorov D. & Silk J. 2010, ApJ, 725, L131
- [142] Ravera L., Barret D., den Herder J. W. et al. 2014, SPIE Conf. Ser., 9144, 2
- [143] Refregier A. 2003, ARA&A, 41, 645
- [144] Reid B. A., Percival W. J., Eisenstein D. J. et al. 2010, MNRAS, 404, 60
- [145] Riemer-Sørensen S. 2014, [arXiv:1405.7943]
- [146] Riemer-Sørensen S. & Hansen S. H. 2009, A&A, 500, L37
- [147] Riemer-Sørensen S., Hansen S. H. & Pedersen K. 2006, ApJ, 644, L33
- [148] Riemer-Sørensen S., Pedersen K., Hansen S. H. & Dahle H. 2007, Phys. Rev. D, 76, 043524
- [149] Riemer-Sørensen S., Wik D., Madejski G. et al. 2015, ApJ, 810, 48
- [150] Romano D., Karakas A. I., Tosi M. & Matteucci F. 2010, A&A, 522, A32
- [151] Roos M. 2012, J. Mod. Phys., 3, 1152
- [152] Rozo E., Wechsler R. H., Rykoff E. S. et al. 2010, ApJ, 708, 645
- [153] Ruchayskiy O., Boyarsky A., Iakubovskiy D. et al. 2016, MNRAS, 460, 1390
- [154] Rudakovskiy A. & Iakubovskiy D. 2016, JCAP, 6, 017
- [155] Sarazin C. L. 1986, Rev. Mod. Phys., 58, 1
- [156] Schneider A. 2015, MNRAS, 451, 3117
- [157] Schneider A. 2016, [arXiv:1601.07553]
- [158] Schutz K. & Slatyer T. R. 2015, JCAP, 1, 021
- [159] Sekiya N., Yamasaki N. Y. & Mitsuda K. 2015, PASJ, 68, S31
- [160] Seljak U., Makarov A., McDonald P. & Trac H. 2006, Phys. Rev. Lett., 97, 191303
- [161] Shao S., Gao L., Theuns T. & Frenk C. S. 2013, MNRAS, 430, 2346
- [162] Shi X. & Fuller G. M. 1999, Phys. Rev. Lett., 82, 2832
- [163] Smith M. C., Ruchti G. R., Helmi A. et al. 2007, MN-

- RAS, 379, 755
- [164] Smith R. K., Brickhouse N. S., Liedahl D. A. & Raymond J. C. 2001, ApJ, 556, L91
- [165] Sonbas E., Rangelov B., Kargaltsev O. et al. 2015, [arXiv:1505.00216]
- [166] Speckhard E. G., Ng K. C. Y., Beacom J. F. & Laha R. 2015, [arXiv:1507.04744]
- [167] Strüder L., Briel U., Dennerl K. et al. 2001, A&A, 365, L18
- [168] Takahashi T., Mitsuda K., Kelley R. et al. 2014, SPIE Conf. Ser., 9144, 25
- [169] Tamura T., Iizuka R., Maeda Y., Mitsuda K. & Yamasaki N. Y. 2015, PASJ, 67, 23
- [170] Tinker J. L., Sheldon E. S., Wechsler R. H. et al. 2012, ApJ, 745, 16
- [171] Tremaine S. & Gunn J. E. 1979, Phys. Rev. Lett., 42, 407
- [172] Turner M. J. L., Abbey A., Arnaud M. et al. 2001, A&A, 365, L27
- [173] Urban O., Werner N., Allen S. W. et al. 2015, MNRAS, 451, 2447
- [174] Venumadhav T., Cyr-Racine F.-Y., Abazajian K. N. & Hirata C. M. 2015, [arXiv:1507.06655]
- [175] Viel M., Becker G. D., Bolton J. S. & Haehnelt M. G. 2013, Phys. Rev. D, 88, 043502
- [176] Viel M., Becker G. D., Bolton J. S. et al. 2008, Phys. Rev. Lett., 100, 041304
- [177] Viel M., Lesgourgues J., Haehnelt M. G., Matarrese S. & Riotto A. 2005, Phys. Rev., D71, 063534
- [178] Viel M., Lesgourgues J., Haehnelt M. G., Matarrese S. & Riotto A. 2006, Phys. Rev. Lett., 97, 071301
- [179] Walker M. 2013, in *Planets, Stars and Stellar Systems. Volume 5: Galactic Structure and Stellar Populations*, 1039
- [180] Wang M.-Y., Strigari L. E., Lovell M. R., Frenk C. S. & Zentner A. R. 2016, MNRAS, 457, 4248
- [181] Watson C. R., Beacom J. F., Yüksel H. & Walker T. P. 2006, Phys. Rev. D, 74, 033009
- [182] Watson C. R., Li Z. & Polley N. K. 2012, JCAP, 3, 18
- [183] Weisskopf M. C., Tananbaum H. D., Van Speybroeck L. P. & O'Dell S. L. 2000, in *X-Ray Optics, Instruments, and Missions III*, eds.: Truemper J. E. & Aschenbach B., 2
- [184] White S. D. M., Frenk C. S. & Davis M. 1983, ApJ, 274, L1
- [185] Yüksel H., Beacom J. F. & Watson C. R. 2008, Phys. Rev. Lett., 101, 121301
- [186] Zandanel F., Weniger C. & Ando S. 2015, JCAP, 9, 060
- [187] Zane S., Walton D., Kennedy T. et al. 2014, SPIE Conf. Ser., 9144, 2
- [188] Zwicky F. 1933, Helvetica Physica Acta, 6, 110

Table 1: Summary of searches for dark matter decay line in X-ray observations conducted so far. This Table is an update of Table 1 in [134].

Ref.	Object	Instrument	Cleaned exposure, ks
[34]	Diffuse X-ray background	HEAO-1, <i>XMM-Newton</i> /EPIC	224, 1450
[35]	Coma, Virgo	<i>XMM-Newton</i> /EPIC	20, 40
[36]	Large Magellanic Cloud	<i>XMM-Newton</i> /EPIC	20
[147]	Milky Way	<i>Chandra</i> /ACIS-S3	Not specified
[181]	M31 (central 5')	<i>XMM-Newton</i> /EPIC	35
[148]	Abell 520	<i>Chandra</i> /ACIS-S3	67
[37]	Milky Way, Ursa Minor	<i>XMM-Newton</i> /EPIC	547, 7
[5]	Milky Way	<i>Chandra</i> /ACIS	1500
[42]	1E 0657-56 ("Bullet cluster")	<i>Chandra</i> /ACIS-I	450
[26]	Milky Way	X-ray micro-calorimeter	0.1
[185]	Milky Way	INTEGRAL/SPI	5500
[30]	M31 (central 5 – 13')	<i>XMM-Newton</i> /EPIC	130
[33]	Milky Way	INTEGRAL/SPI	12200
[114]	Ursa Minor	<i>Suzaku</i> /XIS	70
[146]	Draco	<i>Chandra</i> /ACIS-S	32
[112]	Willman 1	<i>Chandra</i> /ACIS-I	100
[41]	M31, Fornax, Sculptor	<i>XMM-Newton</i> /EPIC , <i>Chandra</i> /ACIS	400, 50, 162
[128]	Willman 1	<i>Chandra</i> /ACIS-I	100
[127]	Segue 1	Swift/XRT	5
[22]	M33	<i>XMM-Newton</i> /EPIC	20-30
[182]	M31 (12 – 28' off-centre)	<i>Chandra</i> /ACIS-I	53
[113]	Willman 1	<i>XMM-Newton</i> /EPIC	60
[107]	Ursa Minor, Draco	<i>Suzaku</i> /XIS	200, 200
[91]	Stacked galaxies	<i>XMM-Newton</i> /EPIC	8500
[89]	M31	<i>Chandra</i> /ACIS-I	404
[120]	Stacked dSphs	<i>XMM-Newton</i> /EPIC	410
[9]	Stacked galaxies	<i>XMM-Newton</i> /EPIC, <i>Chandra</i> /ACIS-I	14600, 15000
[169]	Perseus	<i>Suzaku</i> /XIS	520
[90, 136]	Milky Way	Fermi/GBM	4600
[159]	Milky Way	<i>Suzaku</i> /XIS	31500
[165]	Draco	<i>XMM-Newton</i> /EPIC	87
[149]	1E 0657-56 ("Bullet cluster")	NuSTAR	266
[98]	Draco	<i>XMM-Newton</i> /EPIC	1660

Table 2: Properties of the  $\sim 3.5$  keV line reported by [39, 45]. For their analysis, the authors of [39, 45] use different X-ray datasets observed by MOS [172] and PN [167] cameras on-board *XMM-Newton* observatory [95] and ACIS instrument [81] on-board *Chandra* observatory [183]. All error bars are at  $1\sigma$  (68%) level.

Ref.	Object	Redshift	Instrument	Exposure, Ms	Line position, keV	Line flux, $10^{-6}$ ph/s/cm <sup>2</sup>
[45]	Full stacked sample	0.009-0.354	MOS	6	$3.57 \pm 0.02$	$4.0 \pm 0.8$
[45]	Full stacked sample	0.009-0.354	PN	2	$3.51 \pm 0.03$	$3.9^{+0.6}_{-1.0}$
[45]	Coma+Centaurus+Ophiuchus	0.009-0.028	MOS	0.5	$3.57^a$	$15.9^{+3.4}_{-3.8}$
[45]	Coma+Centaurus+Ophiuchus	0.009-0.028	PN	0.2	$3.57^a$	$< 9.5$ (90%)
[45]	Perseus ( $< 12'$ )	0.016	MOS	0.3	$3.57^a$	$52.0^{+24.1}_{-15.2}$
[45]	Perseus ( $< 12'$ )	0.016	PN	0.05	$3.57^a$	$< 17.7$ (90%)
[45]	Perseus (1 – 12')	0.016	MOS	0.3	$3.57^a$	$21.4^{+7.0}_{-6.3}$
[45]	Perseus (1 – 12')	0.016	PN	0.05	$3.57^a$	$< 16.1$ (90%)
[45]	Rest of the clusters	0.012-0.354	MOS	4.9	$3.57^a$	$2.1^{+0.4}_{-0.5}$
[45]	Rest of the clusters	0.012-0.354	PN	1.8	$3.57^a$	$2.0^{+0.3}_{-0.5}$
[45]	Perseus ( $> 1'$ )	0.016	ACIS-S	0.9	$3.56 \pm 0.02$	$10.2^{+3.7}_{-3.5}$
[45]	Perseus ( $< 9'$ )	0.016	ACIS-I	0.5	$3.56^a$	$18.6^{+7.8}_{-8.0}$
[45]	Virgo ( $< 500''$ )	0.003-0.004	ACIS-I	0.5	$3.56^a$	$< 9.1$ (90%)
[39]	M31 ( $< 14'$ )	$-0.001^b$	MOS	0.5	$3.53 \pm 0.03$	$4.9^{+1.6}_{-1.3}$
[39]	M31 (10 – 80')	$-0.001^b$	MOS	0.7	3.50-3.56	$< 1.8$ ( $2\sigma$ )
[39]	Perseus (23 – 102')	$0.0179^b$	MOS	0.3	$3.50 \pm 0.04$	$7.0 \pm 2.6$
[39]	Perseus (23 – 102')	$0.0179^b$	PN	0.2	$3.46 \pm 0.04$	$9.2 \pm 3.1$
[39]	Perseus, 1st bin (23 – 37')	$0.0179^b$	MOS	0.2	$3.50^a$	$13.8 \pm 3.3$
[39]	Perseus, 2nd bin (42 – 54')	$0.0179^b$	MOS	0.1	$3.50^a$	$8.3 \pm 3.4$
[39]	Perseus, 3rd bin (68 – 102')	$0.0179^b$	MOS	0.03	$3.50^a$	$4.6 \pm 4.6$
[39]	Blank-sky	—	MOS	7.8	3.45-3.58	$< 0.7$ ( $2\sigma$ )

<sup>a</sup> The line position is fixed at given value.

<sup>b</sup> The redshift is fixed at NASA Extragalactic Database (NED) value.

Table 3: Properties of  $\sim 3.5$  keV line searched after February 2014 in different X-ray datasets observed by MOS [172] and PN [167] cameras on-board *XMM-Newton* observatory [95], ACIS [81] instrument on-board *Chandra* observatory [183] and XIS instrument [105] on-board *Suzaku* observatory [129]. All error bars are at  $1\sigma$  (68%) level.

Ref.	Object	Redshift	Instrument	Exposure, Ms	Line position, keV	Line flux, $10^{-6}$ ph/s/cm <sup>2</sup>
[145]	Galactic centre (2.5 – 12')	0.0	ACIS-I	0.8	3.51	$\simeq 10^a$
[97]	Galactic centre (0.3 – 15')	0.0	MOS	0.7	3.51	$45 \pm 4^a$
[97]	Galactic centre (0.3 – 15')	0.0	PN	0.5	3.51	$39 \pm 7^a$
[97]	M31	0.0	MOS	0.5	$3.53 \pm 0.07$	$2.1 \pm 1.5^c$
[27]	Galactic centre (< 14')	0.0	MOS	0.7	$3.539 \pm 0.011$	$29 \pm 5$
[173]	Perseus core (< 6')	$0.0179^b$	XIS	0.74	$3.510_{-0.008}^{+0.023}$	$32.5_{-4.3}^{+3.7}$
[173]	Perseus confined (6 – 12.7')	$0.0179^b$	XIS	0.74	$3.510_{-0.008}^{+0.023}$	$32.5_{-4.3}^{+3.7}$
[173]	Coma (< 12.7')	$0.0231^b$	XIS	0.164	$\simeq 3.45^d$	$\simeq 30^d$
[173]	Ophiuchus (< 12.7')	$0.0280^b$	XIS	0.083	$\simeq 3.45^d$	$\simeq 40^d$
[173]	Virgo (< 12.7')	$0.0036^b$	XIS	0.09	$3.55^a$	$< 6.5$ ( $2\sigma$ )
[93]	Abell 85 (< 14')	$0.0551^b$	MOS	0.20	$3.44_{-0.05}^{+0.06}$	$6.3_{-3.6}^{+3.9}$
[93]	Abell 2199 (< 14')	$0.0302^b$	MOS	0.13	$3.41_{-0.04}^{+0.04}$	$10.1_{-4.8}^{+5.1}$
[93]	Abell 496 (< 14')	$0.0329^b$	MOS	0.13	$3.55_{-0.09}^{+0.06}$	$7.5_{-4.4}^{+6.1}$
[93]	Abell 496 (< 14')	$0.0329^b$	PN	0.08	$3.45_{-0.03}^{+0.04}$	$16.8_{-6.4}^{+5.9}$
[93]	Abell 3266 (< 14')	$0.0589^b$	PN	0.06	$3.53_{-0.06}^{+0.04}$	$8.7_{-4.5}^{+5.1}$
[93]	Abell S805 (< 14')	$0.0139^b$	PN	0.01	$3.63_{-0.06}^{+0.05}$	$17.1_{-7.4}^{+9.3}$
[93]	Coma (< 14')	$0.0231^b$	MOS	0.17	$3.49_{-0.05}^{+0.04}$	$23.7_{-9.0}^{+10.7}$
[93]	Abell 2319 (< 14')	$0.0557^b$	MOS	0.08	$3.59_{-0.06}^{+0.05}$	$18.6_{-7.4}^{+10.7}$
[93]	Perseus (< 14')	$0.0179^b$	MOS	0.16	$3.58_{-0.08}^{+0.05}$	$25.2_{-12.6}^{+12.5}$
[93]	Virgo <sup>e</sup> (< 14')	$0.0036^b$	PN	0.06	—	$< 9.3$
[153]	Draco (< 14')	0.0	PN	0.65	$3.54_{-0.05}^{+0.06}$	$1.65_{-0.70}^{+0.67}$
[77]	Perseus (< 8.3')	$0.0179^b$	XIS	1.67	$3.54 \pm 0.01$	$27.9_{-3.5}^{+3.5}$
[77]	Perseus (< 2')	$0.0179^b$	XIS	1.67	$3.51 \pm 0.02$	$9.3_{-2.7}^{+2.6}$
[77]	Perseus (2' – 4.5')	$0.0179^b$	XIS	1.67	$3.55 \pm 0.02$	$16.7_{-3.0}^{+2.9}$
[77]	Perseus (4.5' – 8.3')	$0.0179^b$	XIS	1.67	$3.58 \pm 0.02$	$16.1_{-3.4}^{+3.2}$
[47]	Stacked clusters	0.01-0.45	XIS	8.1	$3.54^f$	$1.0_{-0.5}^{+0.5}$

<sup>a</sup> Best-fit line flux at the fixed position 3.51 keV coincides with the brightest K XVIII line.

<sup>b</sup> Redshift was fixed at the NASA Extragalactic Database (NED) value.

<sup>c</sup> The line is detected at < 90% confidence level. Such a low flux (compared with [39]) is because of non-physically enhanced level of continuum in the 3-4 keV band used in [97], see [28] for details.

<sup>d</sup> Parameters estimated from Fig. 3 of [173].

<sup>e</sup> Gives an example of the new line non-detection, see Table II of [93] for more details.

<sup>f</sup> Line position is fixed at the best-fit energy detected in *Suzaku* observations of the Perseus cluster by [77].